# CUSTOMIZING MEMS DESIGNS VIA CONDITIONAL GENERATIVE ADVERSARIAL NETWORKS

*Fanping Sui*[†]*, Ruiqi Guo*[†]*, Wei Yue, Kamyar Behrouzi, and Liwei Lin*
Department of Mechanical Engineering, University of California, Berkeley, USA
[†]Fanping Sui and Ruiqi Guo contributed equally to this work.

2022 IEEE 35th International Conference on Micro Electro Mechanical Systems Conference (MEMS) | 978-1-6654-0911-7/22/$31.00 ©2022 IEEE | DOI: 10.1109/MEMS51670.2022.9699476

## ABSTRACT

We present a novel systematic MEMS structure design approach based on a "deep conditional generative model". Utilizing the conditional generative adversarial network (CGAN) on a case study of circular-shaped MEMS resonators, three major advancements have been demonstrated: 1) a high-throughput vectorized MEMS design generation scheme that satisfies the geometric constraints; 2) MEMS structural customization toward tunable, desired physical properties with excellent generation accuracy; and 3) experience-free design space explorations to achieve extreme physical properties, such as low anchor loss of micro resonators. Excellent agreements with experimental data, numerical simulations, and a previously reported machine learning-based analyzer are achieved for validation of our methodology. As such, the proposed scheme could open up a new class of data-driven, intelligent design systems for a wide range of MEMS applications.

## KEYWORDS

MEMS Design, Conditional Generative Adversarial Networks, Data-Driven Design, Machine Learning

## INTRODUCTION

The modern machine learning (ML) technology has become a scientific endeavor in the past decades and has been profoundly changing many sectors of society, including science, technology, and commerce [1]. The ML algorithms are designed to automatically improve themself with experience. In this regard, the ML tools can be applied to the field of design and enable the intelligent, data-driven design space exploration techniques. In the past few years, ML-based design approaches have demonstrated great potentials in automating design processes without the strong dependence on the human intuition or expertise in the related areas [2, 3].

In the field of MEMS, ML algorithms have been used to significantly accelerate the computation speed of MEMS structure properties with decent accuracy as a potential alternative to common computational tools such as the finite element analysis (FEA) [4]. Such supervised learning-based methods enable the low-cost design screening in large and complex design spaces. Although these methods have demonstrated the capability in analyzing the essential properties of MEMS structures and have shown some pioneering results in the data-driven design field, there is still a gap between fitting the design-property trends for prediction and creating new high-performance designs. Recently, a topic that merits more attention is how to generate new MEMS structures autonomously and efficiently with desired (or extreme) properties under the direct guidance of ML.

On the other hand, the generative networks based inverse design methods [5-10], which directly suggest the candidate structures based on desired physical properties, have become an emerging field of study in recent years. Generative adversarial network (GAN) is one of the most commonly used generative models, which is good at proposing candidate designs similar to the training dataset. However, the standard GAN approach has no control over the modes of the patterns, which results in low sample efficiency or separate specialized training when generating structures with different targeted properties [11].

Here, a new deep learning framework - conditional generative adversarial network (CGAN) is developed to generate MEMS designs with customizable properties without the additional training procedures. As shown in Figure 1, by providing the targeted physical properties such as frequency and anchor loss as inputs, the CGAN can propose the pixelated images of candidate designs as outputs, which can be translated to the desired MEMS device designs. The proposed system shows a remarkable generation accuracy (~93.1%) in terms of target frequencies and significant design optimization performances by lowering the anchor losses. We envision that similar data-driven inverse design methods can be applied to other types of MEMS designs such as energy harvesters, accelerometers, and gyroscopes in the future.

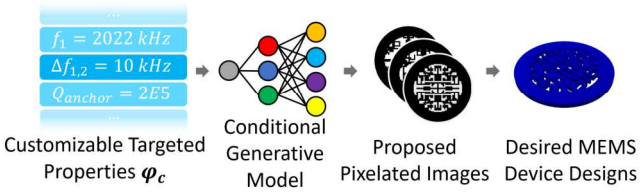


*Figure 1: Schematic diagram of procedures to customize MEMS designs by the proposed conditional generative adversarial network (CGAN). Customizable targeted properties are assigned to the pretrained model and pixelated images representing the desired MEMS designs are generated.*

## SYSTEM ARCHITECTURE

As illustrated in Figure 2A, disk-shaped polysilicon MEMS resonators with center supports are utilized as a case study. The geometric features and material properties of the resonators are identical to the previous works [4, 12], where the Young's modulus of the material (polysilicon) $E$ is $150\ \text{GPa}$, density $\rho$ is $2.3 \times 10^3\ \text{kg/m}^3$, and the Poisson's ratio $\nu$ is $0.29$. The outer ring and inner ring diameters of the structural layer are set as $44\ \mu\text{m}$ and $30.8\ \mu\text{m}$, respectively, and the thickness of the structural layer is $2\ \mu\text{m}$. The anchor stem has a diameter of $2.64\ \mu\text{m}$ and thickness of $0.7\ \mu\text{m}$. As shown in Figures 2B-E, the four modes of interest are the rotational mode, torsional mode along X-direction, torsional mode along Y-direction, and flexural mode, respectively. The physical properties, such

as frequency and anchor loss of the resonator structures for specific resonant modes are analyzed from the commercial FEA software ABAQUS and assumed as the ground truth for evaluations.

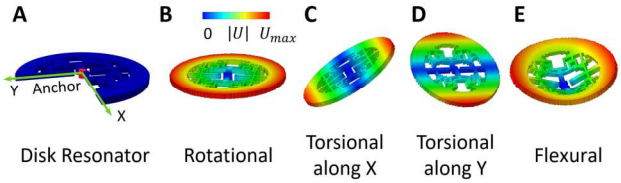


*Figure 2: **A)** Geometry and **B-E)** four vibrational modes of interest of a representative MEMS disk resonator. The color gradients indicate the magnitude of the relative displacements U of the four mode shapes.*

The data-driven inverse design of resonator structures faces two major challenges: 1) computer-generated designs need to satisfy the geometric validity, which ensures all the solid entities of structures to be connected together; 2) the physical properties of generated structures should be tuned conditioned upon input design parameters. As the core controlling unit of the system, the CGAN algorithm can generate candidate designs that satisfy both rubrics simultaneously. As shown in Figures 3A-C, the CGAN architecture has three basic modules with different functionalities: generator $G$, discriminator $D$, and predictor $Q$. The generator and discriminator form a standard GAN and are updated alternately to ensure the geometrical similarities between training samples and newly generated candidates. The predictor is pretrained to map the geometries with physical properties. During the forward pattern generation process, the system takes a random vector $z$, and the targeted physical property requirement $\varphi_c$ for the MEMS structure as inputs. The fully connected decoder $H$ will decode $\varphi_c$ into a higher dimensional vector $c$. Afterwards, the random vector $z$ is concatenated with $c$ to ensure the random variations are introduced in the generative model. Finally, the newly formed vector is transformed to a binary pixel-wise representation of the candidate patterns $\hat{x}$, while satisfying both the $\varphi_c$ condition and geometrical validity through the 2D deconvolution process in the generator.

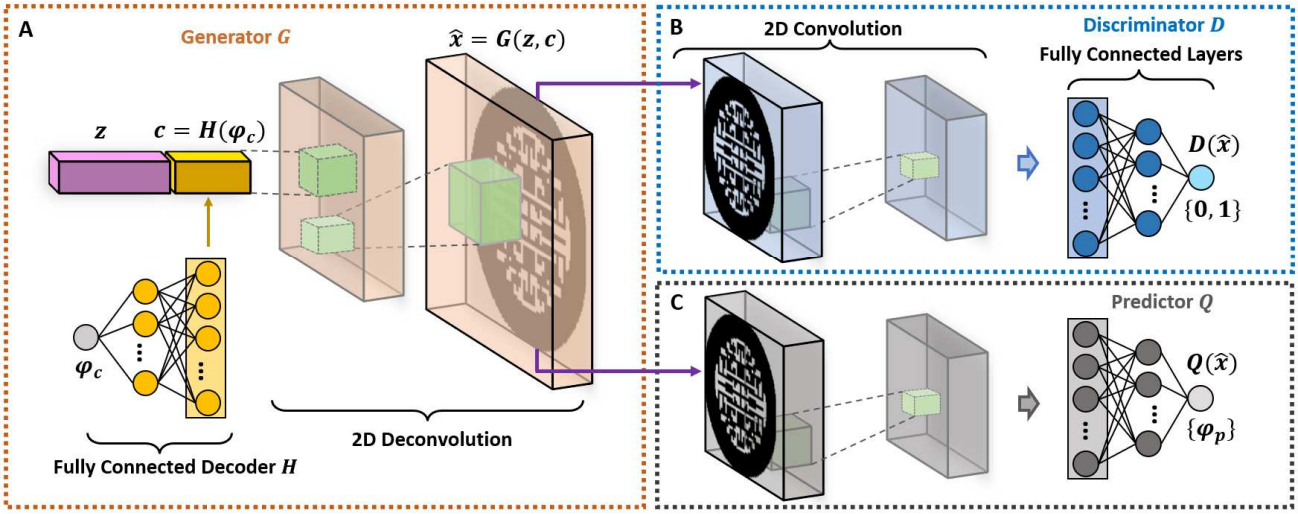


*Figure 3: The system architecture of the CGAN-based MEMS structure designer. **A)** Desired property $\varphi_c$ is decoded to a higher dimensional vector $c$ with the fully connected decoder $H$. The vector $c$ is concatenated with a random vector $z$ as a new vector and fed to the 2D deconvolution generator $G$ to obtain the vectorized pattern $\hat{x}$. **B)** The discriminator $D$ takes $\hat{x}$ as the input which is processed through 2D convolutional and fully connected layers, and the output would be a logical vector that indicates the geometrical validity of the structure. **C)** The predictor $Q$ has similar 2D convolutional layers to $D$ and outputs the predicted property $\varphi_p$ through the architecturally different fully connected layers.*

During the training process, the randomly generated resonator patterns from random Brownian motion processes similar to the previous work [4] have been prepared as the training dataset, where those geometries are connected regions. The patterns from the entire training dataset are labeled as logical true while the generated patterns from the generator are labeled as logical false. The discriminator takes a mixed dataset of sample inputs and justifies whether it is from the training dataset or CGAN-generated dataset, which is realized by a dimensionality reduction process via the 2D convolution layers and fully connected layers. The classification results from the discriminator are compared with the labels and the resulting loss gradients are backpropagated to update the network weights of both the generator and discriminator. The adversarial behavior of the generator-discriminator set promotes the geometrical validity of generated patterns, as the generator can capture the identical geometric features shared among the training dataset. The desired physical properties of generated samples can be achieved by the second trail of the training thread for the fully connected decoder, which is synchronized with the training process of generator-discriminator set. On this thread, the predicted physical properties $\varphi_p$ of the generated patterns are obtained from the pretrained high-throughput predictor. Next, by comparing $\varphi_p$ with $\varphi_c$, the network weights for the fully connected decoder are updated based on the corresponding loss gradients. After sufficient iterations, the generator would be ready for deployment with all the optimized neural network weights frozen.

## RESULTS AND DISCUSSION

The training process of the CGAN framework is illustrated in Figure 4, which takes a total number of 2,500 epochs. The loss curves of the generator-discriminator set are shown in Figure 4A. As the generator and discriminator are competing against each other, their losses are converging to some constants. Figure 4B shows the loss curves of the predictor and decoder and both are converging to zero, indicating that CGAN is realizing the forward interpretation of geometrical designs and inverse translation of physical properties with increasing accuracy. The snapshots of the generator output design patterns with the epoch numbers of 2, 77, 477, 1364, 2020, 2438 are shown in the stages of I-VI of Figure 4C, respectively. It is found that the number of isolated islands in the design configuration is reduced during the training process, indicating that the geometrical validity is progressively enhanced.

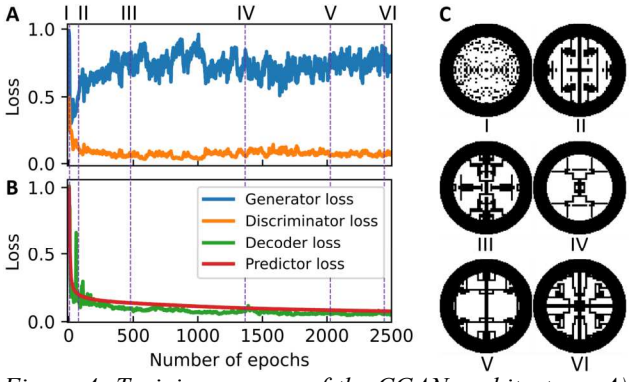


*Figure 4: Training process of the CGAN architecture. **A)** The loss curves of the generator and discriminator. **B)** The loss curves of the decoder and predictor. **C)** The design patterns proposed at different numbers of epochs with geometrical validity enhancements progressively.*

The experimental validations of the proposed CGAN are implemented for the predictive and generative components of the framework. We utilize the identical dataset to the previous work [4] as the training set for the predictor. The prediction results from the properly trained model have exhibited great agreements with experimental data [12], FEA simulations, and the ML-based analyzer [4] as shown in the lower portion of Figure 5. The generative function of CGAN is validated by demonstrating the capability of recovering the original designs with their physical properties as inputs. As shown in the dashed blue boxes in Figure 5, some proposed designs that are highly similar to the original are found in the CGAN-generated design sets.

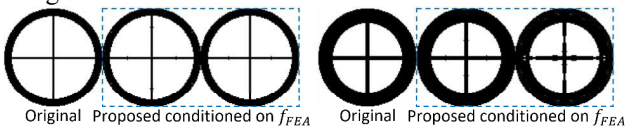


$f_{exp}$ = 24.37 MHz $f_{res}$ = 24.27 MHz
$f_{FEA}$ = 24.33 MHz $f_{pre}$ = 24.40 MHz

$f_{exp}$ = 72.07 MHz $f_{res}$ = 71.97 MHz
$f_{FEA}$ = 72.13 MHz $f_{pre}$ = 72.32 MHz

*Figure 5: Two MEMS resonator designs with 121.8 μm (left) and 44 μm (right) in diameter from the experimental work [12] for validating the predictive and generative functions of the proposed CGAN. $f_{exp}$, $f_{res}$, $f_{FEA}$ and $f_{pre}$ are results from references [12], [4], the FEA simulation and the predictor in this work, respectively. The design patterns in the dashed blue boxes are several representative designs from the generative model that are very similar to the original designs.*

Figure 6 shows several representative designs generated from the proposed CGAN conditioned on the different targeted frequencies of the torsional mode along X-direction. The true frequencies of the output designs are closely matched with targeted frequencies as the generator has learned the underlying regularities to generate designs with the right targeted frequency by manipulating the corresponding pixels.

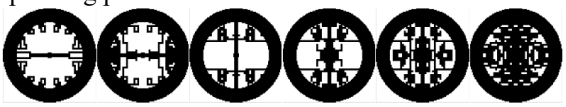

$f_{Tar}$: 0.622 MHz 1.16 MHz 1.61 MHz 2.09 MHz 2.31 MHz 2.51 MHz
$f_{Gen}$: 0.621 MHz 1.15 MHz 1.60 MHz 2.08 MHz 2.30 MHz 2.53 MHz

*Figure 6: Designs generated from the proposed framework with the true frequencies $f_{Gen}$ conditioned on various targeted frequencies $f_{Tar}$.*

The generation performance of the proposed CGAN framework is evaluated by calculating how accurately the conditional generative model outputs designs for achieving the varied input targeted physical properties. The accuracy is defined as $|(\varphi_c - \varphi_p)|/\varphi_c$, where $\varphi_c$ is the targeted physical value and $\varphi_p$ is the corresponding outcome of the generated design calculated by FEA. As a case study, the FEA validated frequencies of the CGAN-generated structures are compared with the corresponding targeted frequency values for the four vibrational modes of the disk-shaped resonators. The targeted frequency values are assigned according to the normal distributions fitted by the training dataset. As shown in Figures 7A-D, all newly created sample points are located very close to the 45-degree red dashed lines, which represent the fully correct matching results in each case. The corresponding generation accuracy for the four modes are 95.8 ± 3.2 %, 95.1 ± 5.1 %, 87.5 ± 4.0 %, 93.9 ± 5.6 %, respectively.

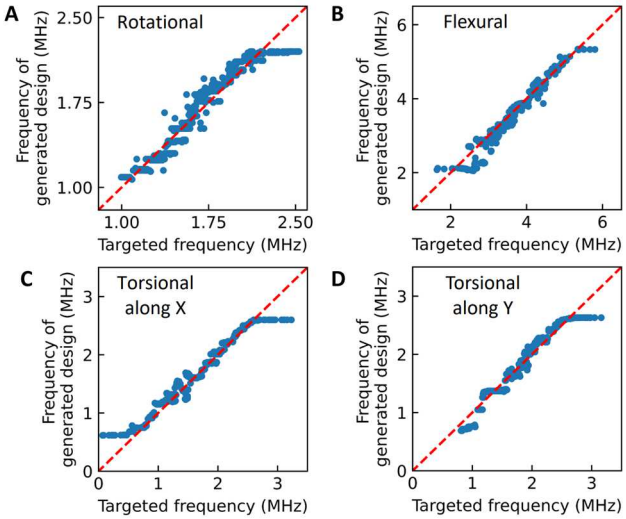


*Figure 7: The targeted frequencies input to the proposed CGAN model with respect to the true frequencies of the generated designs from the FEA simulations for the disk-shaped resonator in **A)** rotational mode, **B)** flexural mode, **C)** the torsional mode along X-direction, **D)** the torsional*

*mode along Y-direction. The red dashed lines in each plot represent 100% accuracy.*

The performance variations would largely depend on the range of the targeted frequencies, which can be reflected from the boundary values in the figures. For example, Figure 7C shows the true frequency of torsional mode along X-direction has an upper bound of 2.6 MHz and a lower bound of 0.6 MHz. Once these outliers are removed, the corresponding generation accuracy can be improved to as high as 94.8 ± 5.6 %. Similar observations can be found for other vibrational modes. The reason is that the geometries with such extreme frequencies are rare, which results in insufficient corresponding training data from the random generation processes.

Design configurations with possible extreme physical properties are also investigated by the proposed CGAN model. For example, the selected physical property of interest is the anchor loss for the resonator devices in the flexural mode $\zeta_{flex}$, which is desirable to be minimized for various applications. As illustrated in Figure 8, the probability distribution of normalized $1/\zeta_{flex}$ of generated samples is compared against that of designs from the training dataset. It is found that CGAN can effectively learn the underlying mechanism of the anchor loss and propose new designs with low anchor losses for higher performances. The key step that facilitates this remarkable optimization performance is by setting an out-of-distribution $1/\zeta_{flex}$ value as the $\varphi_c$ parameter of CGAN framework. As such, the distribution of the CGAN-generated designs is shifted toward the desired direction to achieve ~34% higher performance than the best value from the training dataset.

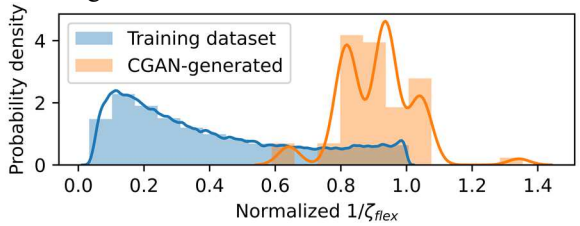


*Figure 8: Distribution comparison between the training dataset (blue color) and CGAN outputs (orange color) for normalized $1/\zeta_{flex}$, where $\zeta_{flex}$ is the anchor loss of the MEMS resonator in the flexural mode. The CGAN-generated designs are not in the distribution of the training dataset and can achieve ~34% improved performance than the best value from the training dataset.*

## CONCLUSION

In this work, we have proposed a novel conditional generative adversarial network framework for the MEMS structural design customizations. The adversarial behavior between the generator and the discriminator enables the generated designs to satisfy the geometrical validity while the decoding and predicting components of the framework secure the desired designs based on the targeted physical properties. High-accuracy design generations and experience-free design space explorations are demonstrated. As a future direction, we will apply this framework to other complicated MEMS design problems targeting specific functionalities.

## ACKNOWLEDGEMENT

The authors appreciate the helpful discussions with Professor Grace X. Gu and Dr. Renxiao Xu regarding the machine learning architecture and FEA simulation setup for anchor loss computation, respectively.

## REFERENCES

[1] M. I. Jordan, T. M. Mitchell, "Machine learning: Trends, perspectives, and prospects", *Science*, vol. 349, pp. 255–260, 2015.

[2] Z. Jin, Z. Zhang, K. Demir, G. X. Gu, "Machine learning for advanced additive manufacturing", *Matter*, vol. 3, pp. 1541–1556, 2020.

[3] F. Sui, R. Guo, Z. Zhang, G. X. Gu, L. Lin, "Deep Reinforcement Learning for Digital Materials Design", *ACS Mater. Lett.*, vol. 3, pp. 1433–1439, 2021.

[4] R. Guo, R. Xu, Z. Wang, F. Sui, L. Lin, "Accelerating MEMS design process through machine learning from pixelated binary images", in *2021 IEEE 34th International Conference on Micro Electro Mechanical Systems (MEMS)*, Virtual, January 25–29, pp. 153–156, 2021.

[5] J. Jiang, D. Sell, S. Hoyer, J. Hickey, J. Yang, J. A. Fan, "Free-form diffractive metagrating design based on generative adversarial networks", *ACS Nano*, vol. 13, pp. 8872–8878, 2019.

[6] B. Kim, S. Lee, J. Kim, "Inverse design of porous materials using artificial neural networks", *Sci. Adv.*, vol. 6, p. eaax9324, 2020.

[7] Y. Mao, Q. He, X. Zhao, "Designing complex architectured materials with generative adversarial networks", *Sci. Adv.*, vol. 6, p. eaaz4169, 2020.

[8] C. T. Chen, G. X. Gu, "Generative deep neural networks for inverse materials design using backpropagation and active learning", *Adv. Sci.*, vol. 7, p. 1902607, 2020.

[9] W. Ma, F. Cheng, Y. Xu, Q. Wen, and Y. Liu, "Probabilistic representation and inverse design of metamaterials based on a deep generative model with semi-supervised learning strategy", *Adv. Mater.*, vol. 31, p. 1901111, 2019.

[10] Z. Yao, B. Sánchez-Lengeling, N. S. Bobbitt, B. J. Bucior, S. G. H. Kumar, S. P. Collins, T. Burns, T. K. Woo, O. K. Farha, R. Q. Snurr, A. Aspuru-Guzik, "Inverse design of nanoporous crystalline reticular materials with deep generative models", *Nat. Mach. Intell.*, vol. 3, pp. 76–86, 2021.

[11] M. Mirza, S. Osindero, "Conditional generative adversarial nets", *arXiv preprint*, arXiv: 1411.1784, 2014.

[12] S. Li, Y. Lin, Y. Xie, Z. Ren, C. Nguyen, "Micromechanical hollow-disk ring resonators", in *17th IEEE International Conference on Micro Electro Mechanical Systems*, Maastricht, January 25–29, pp. 821–824, 2004.

## CONTACT

*F. Sui; +1-510-993-5408; fpsui@berkeley.edu
*R. Guo; +1-510-365-7623; ruiqiguo@berkeley.edu